

UNIVERSIDAD DE CONCEPCIÓN



CENTRO DE INVESTIGACIÓN EN  
INGENIERÍA MATEMÁTICA (CI<sup>2</sup>MA)



A graph-based algorithm for the approximation of the spectrum  
of the curl operator

ANA ALONSO-RODRIGUEZ, JESSIKA CAMAÑO

PREPRINT 2021-28

SERIE DE PRE-PUBLICACIONES



# A GRAPH-BASED ALGORITHM FOR THE APPROXIMATION OF THE SPECTRUM OF THE CURL OPERATOR

A. ALONSO RODRÍGUEZ \* AND J. CAMAÑO †

**Abstract.** We analyze a new algorithm for the finite element approximation of a family of eigenvalue problems for the curl operator that includes, in particular, the approximation of the helicity of a bounded domain. It exploits a tree-cotree decomposition of the graph relating the degrees of freedom of the Lagrangian finite elements and those of the first family of Nédélec finite elements to reduce significantly the dimension of the algebraic eigenvalue problem to be solved. The algorithm is well-adapted to domains of general topology. Numerical experiments, including a non simply connected domain with non connected boundary, are presented in order to assess the performance and generality of the method.

**Key words.** curl operator, eigenvalues and eigenfunctions, Biot-Savart operator, helicity, finite element approximation, tree-cotree decomposition.

**AMS subject classifications.** 65N25, 65N30, 78M10

**1. Introduction.** The spectral problem for the **curl** is relevant in several physical problems. In electromagnetism, a magnetic field  $\mathbf{H}$  that satisfies  $\mathbf{curl} \mathbf{H} = \lambda \mathbf{H}$  for some constant  $\lambda$  is called a linear force-free field. This name comes from the fact that the Lorentz law in linear isotropic media, states that magnetic force  $\mathbf{F}$  is given by  $\mathbf{F} = \mathbf{curl} \mathbf{H} \times \mu \mathbf{H}$  being  $\mu$  the magnetic permeability and, in this case, a magnetic field satisfying  $\mathbf{curl} \mathbf{H} = \lambda \mathbf{H}$  produces a vanishing magnetic force. In plasma physics, it has been proved that a magnetic field  $\mathbf{H}$  which minimizes the magnetic energy with fixed helicity<sup>1</sup> is a linear force-free field. The helicity of a bounded domain  $\Omega$ , a significative quantity in plasma physics<sup>2</sup> (see [12, 13, 5]), can be represented as the minimum of the absolute value of the eigenvalues of the **curl** operator defined on a particular functional space that will be precised in the sequel.

The main mathematical setting for the study of the spectral problem for the **curl** operator is the theory of unbounded operators in Hilbert spaces devising domain of definitions of the **curl** operator where it is self-adjoint. These domains of definition are characterized through appropriate boundary conditions that are strongly dependent on the topology of  $\Omega$ .

Let  $\Omega \subset \mathbb{R}^3$  be a bounded open connected set with Lipschitz continuous boundary  $\Gamma$  and outer unit normal vector  $\mathbf{n}$ . The following Green's formula

$$(1.1) \quad \int_{\Omega} (\mathbf{v} \cdot \mathbf{curl} \mathbf{w} - \mathbf{curl} \mathbf{v} \cdot \mathbf{w}) = \int_{\Gamma} \mathbf{v} \times \mathbf{n} \cdot \mathbf{w},$$

is valid for any regular enough fields  $\mathbf{v}$  and  $\mathbf{w}$ . The choice of the domain of definition of a self-adjoint realization of the **curl** operator is driven by the need of satisfying  $\int_{\Gamma} \mathbf{v} \times \mathbf{n} \cdot \mathbf{w} = 0$ . This is clearly true when acting on vector fields with vanishing tangential components on  $\Gamma$ , namely, satisfying  $\mathbf{v} \times \mathbf{n} = \mathbf{0}$  on  $\Gamma$ . However this condition

---

\*Department of Mathematics, University of Trento, Italy ([ana.alonso@unitn.it](mailto:ana.alonso@unitn.it)).

†Departamento de Matemática y Física Aplicadas, Universidad Católica de la Santísima Concepción and CI<sup>2</sup>MA, Universidad de Concepción, Chile ([jecamano@ucsc.cl](mailto:jecamano@ucsc.cl)).

<sup>1</sup>For a vector field  $\mathbf{v} \in (L^2(\Omega))^3$ , helicity is defined as  $H(\mathbf{v}) = \frac{1}{4\pi} \int_{\Omega} \int_{\Omega} (\mathbf{v}(\mathbf{x}) \times \mathbf{v}(\mathbf{y})) \cdot \frac{\mathbf{x}-\mathbf{y}}{|\mathbf{x}-\mathbf{y}|^3}$ .

<sup>2</sup>The helicity of a bounded domain  $\Omega$  is defined by  $H_{\Omega} = \sup_{\mathbf{v} \in H_0(\text{div}^0; \Omega), \|\mathbf{v}\|_{L^2(\Omega)}=1} |H(\mathbf{v})|$  being

$H_0(\text{div}^0; \Omega) = \{\mathbf{v} \in (L^2(\Omega))^3 : \text{div} \mathbf{v} = 0, \mathbf{v} \cdot \mathbf{n} = 0 \text{ on } \partial\Omega\}$ .

is too strong for the spectral problem since the **curl** operator with boundary condition  $\mathbf{v} \times \mathbf{n} = \mathbf{0}$  has no eigenvalue  $\lambda \neq 0$ . (See, e. g., [5, pp. 5638–5639], [19, Lemma 3]).

If  $\Omega$  is simply connected then the **curl** operator is self-adjoint restricted to the space

$$(1.2) \quad \mathcal{X} := \{ \mathbf{v} \in H(\mathbf{curl}; \Omega) : \mathbf{curl} \mathbf{v} \cdot \mathbf{n} = 0 \text{ on } \Gamma \}.$$

In fact,  $\mathbf{curl} \mathbf{v} \cdot \mathbf{n}$  is the scalar tangential curl of  $\mathbf{v}_\tau := \mathbf{n} \times \mathbf{v} \times \mathbf{n}$  on  $\Gamma$  (see, e.g., [3]). On a simply connected boundary the tangential curl of a tangential field  $\mathbf{v}_\tau$  is zero if and only if it is a tangential gradient. Moreover if a tangential field  $\mathbf{v}_\tau$  is a tangential gradient then  $\mathbf{v}_\tau \times \mathbf{n} = \mathbf{grad}_\tau \phi \times \mathbf{n} = \mathbf{curl}_\tau \phi$ . If both  $\mathbf{v}$  and  $\mathbf{w}$  are in  $\mathcal{X}$  then one has  $\int_\Gamma \mathbf{v} \times \mathbf{n} \cdot \mathbf{w} = \int_\Gamma \mathbf{v}_\tau \times \mathbf{n} \cdot \mathbf{w}_\tau = \int_\Gamma \mathbf{curl}_\tau \phi \cdot \mathbf{grad}_\tau \psi = 0$ .

If  $\Omega$  is not simply connected then the condition  $\mathbf{curl} \mathbf{v} \cdot \mathbf{n} = 0$  is not enough to obtain a self-adjoint realization of the **curl** operator since there are tangential fields with scalar tangential **curl** equal to zero that are not tangential gradients. They are the so-called tangential harmonic fields and they are related with the non-bounding cycles on  $\Gamma$ . So it is necessary to incorporate additional constraints that are related with the first homology group of  $\Gamma$  (see [8]).

In [2] it was studied the variational formulation and numerical approximation of a family of eigenvalue problems of the **curl** operator restricted to appropriate subspaces of  $\mathcal{X}$  where it is self-adjoint. The additional constraints are vanishing line integrals along non-bounding cycles of  $\Gamma$ , namely, along representatives of non trivial elements of the first homology group of  $\Gamma$ . The numerical scheme is based on a saddle point variational formulation of the problem and uses the first family of Nédélec finite elements (see [14]).

In this paper we propose a new implementation of the same numerical scheme. The main novelty is the construction of a basis of the finite element space that leads to a reduced algebraic eigenvalue problem. For finite element spaces of the lowest order this basis can be constructed using a tree-cotree decomposition of the graph defined by the vertices and the edges of the mesh. The construction of the basis can be easily extended to finite element spaces of degree  $r > 1$  using the graph associated to the Lagrangian and the Nédélec moments introduced in [1].

We pay particular attention to the topological generality of  $\Omega$  that could be not simply connected (first Betti number greater than zero) and with non connected boundary (second Betti number greater than zero). We present some numerical experiments for finite elements of degree  $r = 1$  showing that the use of these basis reduces significantly the dimension of the algebraic eigenvalue problem with the consequent saving of computational time. We include a test case where the domain is a toroidal shell, a non simply connected domain with non connected boundary. In particular we approximate the helicity of different toroidal shells.

The paper is organised as follows. Next section contains some preliminary geometrical results. In Section 3 we introduce the family of eigenvalue problems of the **curl** operator that will be considered, its variational formulation and finite elements approximation and we recall the convergence results proved in [2]. In Section 4 we present a new procedure to construct a basis of the finite element spaces that reduce drastically the dimension of the algebraic problem. Section 5 contains numerical experiments to asses the performance and generality of the method.

**2. Some preliminary results.** Let  $\Omega \subset \mathbb{R}^3$  be a bounded open connected set with Lipschitz continuous boundary  $\Gamma$  (either smooth or polyhedral) and outer unit normal vector  $\mathbf{n}$ . Let  $B$  be an open ball containing  $\bar{\Omega}$ . We denote  $\Omega' = B \setminus \Omega$ .

If the second Betti number of  $\Omega$  is equal to  $p \geq 0$  then the boundary  $\Gamma$  of  $\Omega$  has  $p+1$  connected components:  $\Gamma = \bigcup_{s=0}^p \Gamma_s$ . We denote  $\Gamma_0$  the most external one. Each one of these connected components  $\Gamma_s$  divides  $\mathbb{R}^3$  into two connected open regions: a bounded one  $\Omega_s$  and an unbounded one  $\mathbb{R}^3 \setminus \overline{\Omega_s}$ . We denote  $\Omega'_s = B \setminus \overline{\Omega_s}$ . It holds that

$$\Omega = \Omega_0 \cap \Omega'_1 \cap \cdots \cap \Omega'_p \quad \text{and} \quad \Omega' = \Omega'_0 \cup \Omega_1 \cup \cdots \cup \Omega_p.$$

Let  $s \in \{0, 1, \dots, p\}$ : if the first Betti number of  $\Gamma_s$  is equal to  $2g_s \geq 0$  then the first Betti number of both  $\overline{\Omega_s}$  and  $\overline{\Omega'_s}$  is equal to  $g_s \geq 0$ . If  $g_s > 0$  it is possible to consider  $2g_s$  non-bounding connected cycles on  $\Gamma_s$ ,  $\{\gamma_{s,i}\}_{i=1}^{g_s} \cup \{\gamma'_{s,j}\}_{j=1}^{g_s}$ , that are (representative of) the generators of the first homology group of  $\Gamma_s$  and such that:

- $\{\gamma_{s,i}\}_{i=1}^{g_s}$  are (representative of) the generators of the first homology group of  $\overline{\Omega'_s}$ ;
- $\{\gamma'_{s,j}\}_{j=1}^{g_s}$  are (representative of) the generators of the first homology group of  $\overline{\Omega_s}$ ;
- in  $\Omega_s$  there exist  $g_s$  ‘cutting’ surfaces  $\{\Sigma_{s,i}\}_{i=1}^{g_s}$ , that are connected orientable Lipschitz surfaces satisfying  $\Sigma_{s,i} \subset \Omega_s$  and  $\partial\Sigma_{s,i} \subset \Gamma_s$ , such that every curl-free vector in  $\Omega_s$  has a global potential in the ‘cut’ domain  $\Omega_s \setminus \bigcup_{i=1}^{g_s} \Sigma_{s,i}$ ; each surface  $\Sigma_{s,j}$  satisfies  $\partial\Sigma_{s,i} = \gamma_{s,i}$ , ‘cuts’ the corresponding cycle  $\gamma'_{s,i}$  and does not intersect the other cycles  $\gamma'_{s,j}$  for  $j \neq i$ ;
- in  $\Omega'_s$  there exist  $g_s$  ‘cutting’ surfaces  $\{\Sigma'_{s,j}\}_{j=1}^{g_s}$ , that are connected orientable Lipschitz surfaces satisfying  $\Sigma'_{s,j} \subset \Omega'_s$  and  $\partial\Sigma'_{s,j} \subset \Gamma_s$ , such that every curl-free vector in  $\Omega'_s$  has a global potential in the ‘cut’ domain  $\Omega'_s \setminus \bigcup_{j=1}^{g_s} \Sigma'_{s,j}$ ; each surface  $\Sigma'_{s,j}$  satisfies  $\partial\Sigma'_{s,j} = \gamma'_{s,j}$ , ‘cuts’ the corresponding cycle  $\gamma_{s,j}$ , and does not intersect the other cycles  $\gamma_{s,i}$  for  $i \neq j$ .

In particular we can assume that  $\gamma_{s,i} \cap \gamma_{s,j} = \emptyset$  and  $\gamma'_{s,i} \cap \gamma'_{s,j} = \emptyset$  if  $i \neq j$ , while  $\gamma_{s,i}$  intersects  $\gamma'_{s,i}$  just at a point  $P_{s,i}$ .

For each  $i \in \{1, \dots, g_s\}$  we fix a unit normal vector  $\mathbf{n}_{s,i}$  on  $\Sigma_{s,i}$ . By  $\Sigma_{s,i}^+$  and  $\Sigma_{s,i}^-$  we denote the two faces of  $\Sigma_{s,i}$ . For any function  $\phi \in H^1(\Omega_s \setminus \Sigma_{s,i})$  we denote  $[[\phi]]_{\Sigma_{s,i}}$  the jump of  $\phi$  across  $\Sigma_{s,i}$ , namely,  $\phi|_{\Sigma_{s,i}^+} - \phi|_{\Sigma_{s,i}^-}$ . In general, the functions  $\phi \in H^1(\Omega_s \setminus \Sigma_{s,i})$  do not admit an extension to the whole  $\Omega_s$  that lies in the space  $H^1(\Omega_s)$ . However, any extension of  $\mathbf{grad} \phi$  obviously belongs to  $[L^2(\Omega_s)]^3$ . We denote  $\widetilde{\mathbf{grad} \phi}$  such an extension.

The choice of the unit normal vector  $\mathbf{n}_{s,i}$  on  $\Sigma_{s,i}$  induces a *right hand* orientation on  $\partial\Sigma_{s,i} = \gamma_{s,i}$ . We denote  $\mathbf{t}_{s,i}$  the corresponding unit tangent vector. Moreover we denote  $\mathbf{t}'_{s,i}$  the unit tangent vector on  $\gamma'_{s,i}$  such that

$$\oint_{\gamma'_{s,i}} \widetilde{\mathbf{grad} \phi} \cdot \mathbf{t}'_{s,i} = [[\phi]]_{\Sigma_{s,i}}$$

for any  $\phi \in H^1(\Omega_s \setminus \Sigma_{s,i})$  regular enough on  $\Gamma_s$ . Then we choose the unit normal vector  $\mathbf{n}'_{s,i}$  on  $\Sigma'_{s,i}$  according with this choice of  $\mathbf{t}'_{s,i}$ . It is worth noting that if  $\phi' \in H^1(\Omega'_s \setminus \Sigma'_{s,i})$  is regular enough on  $\Gamma_s$  then

$$\oint_{\gamma_{s,i}} \widetilde{\mathbf{grad} \phi'} \cdot \mathbf{t}_{s,i} = [[\phi']]_{\Sigma'_{s,i}}.$$

Figure 1 shows an example of consistent orientation of the cutting surfaces for a toroidal surface  $\Gamma_s$ .

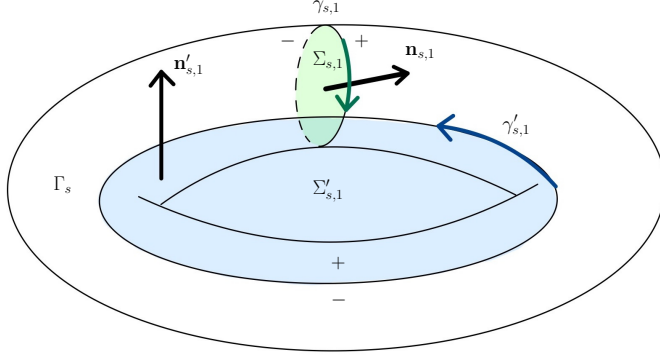


FIG. 1. The oriented cycles and cutting surfaces of a toroidal surface  $\Gamma_s$ .

If  $\beta_1(\Omega) = g$  and  $\beta_2(\Omega) = p$  are the first Betti number and the second Betti number of  $\Omega$  respectively, then  $g = \sum_{s=0}^p g_s$ . The first Betti number of  $\Gamma = \cup_{s=0}^p \Gamma_s$  is equal to  $2g$  and the non-bounding cycles  $\{\gamma_i\}_{i=1}^g \cup \{\gamma'_i\}_{i=1}^g$  with

$$\{\gamma_i\}_{i=1}^g = \{\gamma_{0,j}\}_{j=1}^{g_0} \cup \{\gamma'_{1,j}\}_{j=1}^{g_1} \cup \cdots \cup \{\gamma'_{p,j}\}_{j=1}^{g_p}$$

and

$$\{\gamma'_i\}_{i=1}^g = \{\gamma'_{0,j}\}_{j=1}^{g_0} \cup \{\gamma_{1,j}\}_{j=1}^{g_1} \cup \cdots \cup \{\gamma_{p,j}\}_{j=1}^{g_p}$$

are (representative of) the generators of the first homology group of  $\Gamma$ . They are such that:

- $\{\gamma_i\}_{i=1}^g$  are (representative of) the generators of the first homology group of  $\mathbb{R}^3 \setminus \Omega$ ;
- $\{\gamma'_j\}_{j=1}^g$  are (representative of) the generators of the first homology group of  $\overline{\Omega}$ .

Clearly  $\gamma_i \cap \gamma_j = \emptyset$  and  $\gamma'_i \cap \gamma'_j = \emptyset$  while  $\gamma_i$  intersects  $\gamma'_i$  just at a point  $P_i$ .

The associated sets of cutting surfaces in  $\Omega$  and  $\Omega'$  are given by

$$\{\Sigma_i\}_{i=1}^g := \{\Sigma_{0,i} \cap \Omega\}_{i=1}^{g_0} \cup \{\Sigma'_{1,i} \cap \Omega\}_{i=1}^{g_1} \cup \cdots \cup \{\Sigma'_{p,i} \cap \Omega\}_{i=1}^{g_p}$$

and

$$\{\Sigma'_j\}_{j=1}^g := \{\Sigma'_{0,j}\}_{j=1}^{g_0} \cup \{\Sigma_{1,j}\}_{j=1}^{g_1} \cup \cdots \cup \{\Sigma_{p,j}\}_{j=1}^{g_p}$$

respectively.

If  $\partial\Omega$  is not connected then  $\partial\Sigma_i$  could be not connected. In such a case  $\gamma_i \neq \partial\Sigma_i$ . However it holds that  $[\gamma_i]_{\mathcal{H}_1(\overline{\Omega'})} = [\partial\Sigma_i]_{\mathcal{H}_1(\overline{\Omega'})}$ , namely, the homology class in  $\overline{\Omega'}$  of  $\gamma_i$  and  $\partial\Sigma_i$  are the same. If  $\partial\Sigma_i$  is not connected then  $\gamma_i$  is one of its connected components. The other connected components of  $\partial\Sigma_i$  are homologically trivial in  $\overline{\Omega'}$ . On the other hand,  $\partial\Sigma'_j = \gamma'_j$ .

Figure 2 shows the cutting surfaces of a toroidal shell and its complementary. In this case  $\partial\Omega$  has two connected components that are two concentric torous. In the figure half of these two toroidal surface are sketched in black. The cutting surfaces of  $\Omega$  are  $\Sigma_1 (= \Sigma_{0,1} \cap \Omega)$ , in green, and  $\Sigma_2 (= \Sigma'_{1,1} \cap \Omega)$  in yellow and the cutting surfaces of  $\Omega'$  are  $\Sigma'_1 (= \Sigma'_{0,1})$ , in blue, and  $\Sigma'_2 (= \Sigma_{1,1})$  in pink. The boundary of  $\Sigma'_1$  and  $\Sigma'_2$  are connected while the boundaries of  $\Sigma_1$  and  $\Sigma_2$  are not. They have two connected

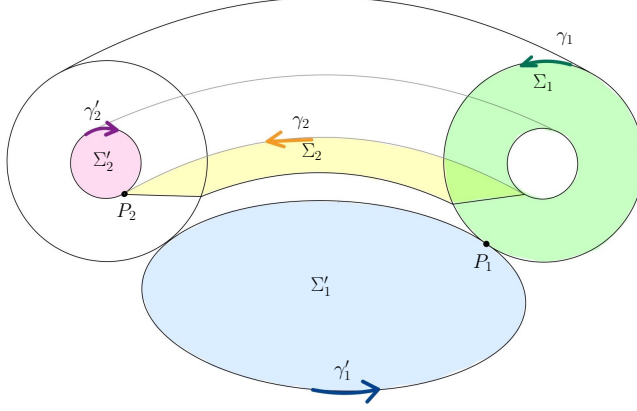


FIG. 2. Half of the toroidal shell and the cutting surfaces in  $\Omega$  (green and yellow) and  $\Omega'$  (blue and pink).

components. One of them is the boundary of a surface in  $\Omega'$ , so homologically trivial in  $\Omega'$ , while the other one,  $\gamma_1$  and  $\gamma_2$  respectively, are homologically non trivial in  $\Omega'$ .

The following lemma gives a representation of a basis of the space

$$\mathcal{K}_T(\Omega) = \{\boldsymbol{\rho} \in [L^2(\Omega)]^3 : \mathbf{curl} \boldsymbol{\rho} = \mathbf{0} \text{ and } \operatorname{div} \boldsymbol{\rho} = 0 \text{ in } \Omega \text{ and } \boldsymbol{\rho} \cdot \mathbf{n} = 0 \text{ on } \Gamma\}$$

of harmonic Neumann fields in  $\Omega$ .

LEMMA 2.1. A basis of the space  $\mathcal{K}_T(\Omega)$  is given by  $\{\boldsymbol{\rho}_i\}_{i=1}^g$  where  $\boldsymbol{\rho}_i := \widetilde{\mathbf{grad}} \phi_i$ ,  $i \in \{1, \dots, g\}$ , and  $\phi_i \in H^1(\Omega \setminus \Sigma_i)/\mathbb{R}$  is the unique solution of

$$\begin{aligned} \Delta \phi_i &= 0 & \text{in } \Omega \setminus \Sigma_i, \\ \partial_{\mathbf{n}} \phi_i &= 0 & \text{on } \partial\Omega, \\ [[\partial_{\mathbf{n}} \phi_i]]_{\Sigma_i} &= 0, \\ [[\phi_i]]_{\Sigma_i} &= 1. \end{aligned}$$

*Proof.* See, for instance, [7, Lemma 1.3].  $\square$

A basis of  $\mathcal{K}_T(\Omega') := \{\mathbf{z} \in [L^2(\Omega')]^3 : \mathbf{curl} \mathbf{z} = \mathbf{0}, \operatorname{div} \mathbf{z} = 0, \text{ and } \mathbf{z} \cdot \mathbf{n} = 0 \text{ on } \Gamma\}$  can be obtained similarly from the set of cutting surfaces  $\{\Sigma'_j\}_{j=1}^g$ . We denote  $\{\boldsymbol{\rho}'_j\}_{j=1}^g$  the corresponding basis of  $\mathcal{K}_T(\Omega')$ .

Following [2] for each  $\mathbf{v} \in \mathcal{X}$  we set, for  $i, j \in \{1, \dots, g\}$

$$(2.1) \quad \begin{aligned} \oint_{\partial\Sigma_i} \mathbf{v} \cdot \mathbf{t}_i &:= \int_{\Omega} \mathbf{curl} \mathbf{v} \cdot \boldsymbol{\rho}_i = \int_{\Gamma} \mathbf{n} \times \mathbf{v} \cdot \boldsymbol{\rho}_i, \\ \oint_{\partial\Sigma'_j} \mathbf{v} \cdot \mathbf{t}'_j &:= \int_{\Omega'} \mathbf{curl} \tilde{\mathbf{v}} \cdot \boldsymbol{\rho}'_j = - \int_{\Gamma} \mathbf{n} \times \mathbf{v} \cdot \boldsymbol{\rho}'_j. \end{aligned}$$

Here  $\tilde{\mathbf{v}}$  is a bounded extension of  $\mathbf{v}$  to  $H(\mathbf{curl}; \mathbb{R}^3)$ .

It has been proved in [2] that for all  $k \in \{1, \dots, g\}$

$$\oint_{\partial\Sigma_i} \boldsymbol{\rho}_k \cdot \mathbf{t}_i = 0 \quad \text{and} \quad \oint_{\partial\Sigma'_j} \boldsymbol{\rho}_k \cdot \mathbf{t}'_j = \delta_{j,k}.$$

**3. Statement of the problem.** Let  $\mathcal{I}$  be a subset of  $G = \{1, \dots, g\}$  and  $\mathcal{I}^c = G \setminus \mathcal{I}$ . For each choice of  $\mathcal{I}$  we can consider the following eigenvalue problem:

Find  $\lambda \in \mathbb{C}$  and  $\mathbf{u} \in [L^2(\Omega)]^3$ ,  $\mathbf{u} \neq \mathbf{0}$ , such that

$$(3.1) \quad \begin{aligned} \mathbf{curl} \mathbf{u} &= \lambda \mathbf{u} && \text{in } \Omega, \\ \mathbf{curl} \mathbf{u} \cdot \mathbf{n} &= 0 && \text{on } \Gamma, \\ \oint_{\partial \Sigma_i} \mathbf{u} \cdot \mathbf{t}_i &= 0 && \forall i \in \mathcal{I}, \\ \oint_{\partial \Sigma'_j} \mathbf{u} \cdot \mathbf{t}'_j &= 0 && \forall j \in \mathcal{I}^c. \end{aligned}$$

Denoting

$$\mathcal{Z}_{\mathcal{I}} = \left\{ \mathbf{v} \in \mathcal{X} : \oint_{\partial \Sigma_i} \mathbf{v} \cdot \mathbf{t}_i = 0 \quad \forall i \in \mathcal{I} \quad \text{and} \quad \oint_{\partial \Sigma'_j} \mathbf{v} \cdot \mathbf{t}'_j = 0 \quad \forall j \in \mathcal{I}^c \right\},$$

the previous eigenvalue problem can be equivalently rewritten as follows:

**Problem 1.** Find  $\lambda \in \mathbb{C}$  and  $\mathbf{u} \in \mathcal{Z}_{\mathcal{I}}$ ,  $\mathbf{u} \neq \mathbf{0}$ , such that

$$(3.2) \quad \mathbf{curl} \mathbf{u} = \lambda \mathbf{u}.$$

REMARK 3.1. From (2.1) it follows that when  $\mathcal{I} = G$ ,

$$\mathcal{Z}_{\mathcal{I}} = \left\{ \mathbf{v} \in \mathcal{X} : \int_{\Omega} \mathbf{curl} \mathbf{v} \cdot \boldsymbol{\rho} = 0 \quad \forall \boldsymbol{\rho} \in \mathcal{K}_T(\Omega) \right\}.$$

This case corresponds to the eigenvalue problem studied in [9], [10], [15], [16], and [20].

Let us denote  $H(\mathbf{curl}^0; \Omega) := \{ \mathbf{v} \in H(\mathbf{curl}; \Omega) : \mathbf{curl} \mathbf{v} = \mathbf{0} \text{ in } \Omega \}$ . Then

$$\mathcal{H}_{\mathcal{I}} := \mathcal{Z}_{\mathcal{I}} \cap H(\mathbf{curl}^0; \Omega)$$

is the eigenspace associated to the zero eigenvalue of (3.2). We consider the following mixed variational problem:

**Problem 2.** Find  $\lambda \in \mathbb{C}$  and  $(\mathbf{u}, \mathbf{q}) \in \mathcal{Z}_{\mathcal{I}} \times \mathcal{H}_{\mathcal{I}}$ ,  $\mathbf{u} \neq \mathbf{0}$ , such that

$$(3.3) \quad \begin{aligned} \int_{\Omega} \mathbf{curl} \mathbf{u} \cdot \mathbf{curl} \bar{\mathbf{v}} + \int_{\Omega} \mathbf{q} \cdot \bar{\mathbf{v}} &= \lambda \int_{\Omega} \mathbf{u} \cdot \mathbf{curl} \bar{\mathbf{v}} && \forall \mathbf{v} \in \mathcal{Z}_{\mathcal{I}}, \\ \int_{\Omega} \mathbf{u} \cdot \bar{\mathbf{p}} &= 0 && \forall \mathbf{p} \in \mathcal{H}_{\mathcal{I}}. \end{aligned}$$

The following result establishes the equivalence between the two previous problems.

LEMMA 3.1. *If  $(\lambda, \mathbf{u})$ ,  $\lambda \neq 0$ , is a solution to Problem 1, then  $(\lambda, \mathbf{u}, \mathbf{0})$  is a solution to Problem 2. If  $(\lambda, \mathbf{u}, \mathbf{q})$  is a solution to Problem 2, then  $\mathbf{q} = \mathbf{0}$  and  $(\lambda, \mathbf{u})$  is a solution to Problem 1.*

*Proof.* See Lemma 8 in [2]. □

The proof of the well-posedness of Problem 1 in [2] is based on the following solution operator  $\mathbf{T} : \mathcal{Z}_{\mathcal{I}} \rightarrow \mathcal{Z}_{\mathcal{I}}$ . For a given  $\mathbf{f} \in \mathcal{Z}_{\mathcal{I}}$ ,  $\mathbf{T}\mathbf{f} = \mathbf{w} \in \mathcal{Z}_{\mathcal{I}}$  and there exists  $\mathbf{q} \in \mathcal{H}_{\mathcal{I}}$  such that

$$\begin{aligned} \int_{\Omega} \mathbf{curl} \mathbf{w} \cdot \mathbf{curl} \bar{\mathbf{v}} + \int_{\Omega} \mathbf{q} \cdot \bar{\mathbf{v}} &= \int_{\Omega} \mathbf{f} \cdot \mathbf{curl} \bar{\mathbf{v}} \quad \forall \mathbf{v} \in \mathcal{Z}_{\mathcal{I}}, \\ \int_{\Omega} \mathbf{w} \cdot \bar{\mathbf{p}} &= 0 \quad \forall \mathbf{p} \in \mathcal{H}_{\mathcal{I}}. \end{aligned}$$

This operator  $\mathbf{T}$  is compact and self-adjoint and its spectrum  $\sigma(\mathbf{T})$  decomposes as  $\{\mu_n\}_{n \in \mathbb{N}} \cup \{0\}$  being  $\{\mu_n\}_{n \in \mathbb{N}}$  a sequence of finite multiplicity eigenvalues which converges to 0, (see [2]). The spectrum of  $\mathbf{T}$  and the solution of Problem 2 are related in the following sense:  $\mathbf{T}\mathbf{u} = \mu\mathbf{u}$  with  $\mathbf{u} \neq \mathbf{0}$  and  $\mu \neq 0$  if and only if  $(\lambda, \mathbf{u}, \mathbf{0})$  is a solution of Problem 2 with  $\lambda = 1/\mu$ .

REMARK 3.2. *If  $\mathcal{I} = \emptyset$  then  $\mathbf{T}$  is the projected Biot-Savart operator  $\widehat{BS}$  defined in [18] (see also [4]). The helicity of  $\Omega$  is  $|\mu_{max}|$ , the maximum of the absolute value of the eigenvalues of  $\widehat{BS}$ .*

**3.1. Finite element approximation.** To introduce a Galerkin approximation of Problem 2 we assume that  $\Omega$  has polyhedral Lipschitz continuous boundary and we choose the ‘cutting’ surfaces  $\Sigma_i$ ,  $i = 1, \dots, g$ , also polyhedral. Let  $\{\mathcal{T}_h\}_{h>0}$  be a regular family of tetrahedral partitions of  $\bar{\Omega}$ . We denote by  $\mathbf{V}_h$ ,  $\mathbf{E}_h$  and  $\mathbf{F}_h$  the set of all the vertices, edges and faces of  $\mathcal{T}_h$  respectively. It is not restrictive to assume that there exist sets  $\mathbf{F}_{\Sigma_i} \subset \mathbf{F}_h$  and  $\mathbf{E}_{\gamma'_j} \subset \mathbf{E}_h$ , for  $j = 1, \dots, g$  such that

$$(3.4) \quad \Sigma_i = \bigcup_{f \in \mathbf{F}_{\Sigma_i}} f \quad \text{and} \quad \partial\Sigma'_j = \gamma'_j = \bigcup_{e \in \mathbf{E}_{\gamma'_j}} e \quad \text{for } j = 1, \dots, g.$$

The mesh parameter  $h$  denotes the maximum diameter of all the tetrahedra  $T \in \mathcal{T}_h$ . For any  $T \in \mathcal{T}_h$  and  $r \geq 1$ , let  $\mathcal{N}^r(T) := \mathbb{P}_{r-1}(T)^3 \oplus \{\mathbf{p} \in \widetilde{\mathbb{P}}_r(T)^3 : \mathbf{p}(\mathbf{x}) \cdot \mathbf{x} = 0\}$ , where  $\mathbb{P}_r$  is the set of polynomials of degree not greater than  $r$  and  $\widetilde{\mathbb{P}}_r$  is the subset of homogeneous polynomials of degree  $r$ . The corresponding global space to approximate  $H(\mathbf{curl}; \Omega)$  is the well-known Nédélec space defined as follows:

$$\mathcal{N}_h^r := \{\mathbf{v}_h \in H(\mathbf{curl}; \Omega) : \mathbf{v}_h \in \mathcal{N}^r(T), \forall T \in \mathcal{T}_h\}.$$

Whence, the natural approximation space for  $\mathcal{Z}_{\mathcal{I}}$  is  $\mathcal{Z}_{\mathcal{I},h} = \mathcal{Z}_{\mathcal{I}} \cap \mathcal{N}_h^r$ , namely,

$$\mathcal{Z}_{\mathcal{I},h} = \left\{ \mathbf{v}_h \in \mathcal{N}_h^r : \mathbf{curl} \mathbf{v}_h \cdot \mathbf{n} = 0 \text{ on } \Gamma, \oint_{\partial\Sigma_i} \mathbf{v}_h \cdot \mathbf{t}_i = 0 \text{ if } i \in \mathcal{I} \right. \\ \left. \text{and } \oint_{\partial\Sigma'_j} \mathbf{v}_h \cdot \mathbf{t}'_j = 0 \text{ if } j \in \mathcal{I}^c \right\}.$$

To discretize the Lagrange multiplier  $\mathbf{q} \in \mathcal{H}_{\mathcal{I}}$  we use the finite element space

$$\mathcal{H}_{\mathcal{I},h} := \mathcal{Z}_{\mathcal{I},h} \cap H(\mathbf{curl}^0; \Omega).$$

Note that

$$(3.5) \quad \mathcal{H}_{\mathcal{I},h} = \left\{ \mathbf{v}_h \in \mathcal{N}_h^r : \mathbf{curl} \mathbf{v}_h = \mathbf{0} \text{ in } \Omega, \text{ and } \oint_{\partial\Sigma'_j} \mathbf{v}_h \cdot \mathbf{t}'_j = 0 \text{ if } j \in \mathcal{I}^c \right\}$$

as  $\oint_{\partial\Sigma_i} \mathbf{v}_h \cdot \mathbf{t}_i = \int_{\Sigma_i} \mathbf{curl} \mathbf{v}_h \cdot \mathbf{n}_i$ ,  $i \in \mathcal{I}$ , and the last integral vanishes as  $\mathbf{curl} \mathbf{v}_h = \mathbf{0}$  in  $\Omega$ .

Now, we are in position to introduce a finite element discretization of Problem 2.

**Problem 3.** Find  $\lambda_h \in \mathbb{C}$  and  $(\mathbf{u}_h, \mathbf{q}_h) \in \mathcal{Z}_{\mathcal{I},h} \times \mathcal{H}_{\mathcal{I},h}$ ,  $\mathbf{u}_h \neq \mathbf{0}$ , such that

$$\begin{aligned} \int_{\Omega} \mathbf{curl} \mathbf{u}_h \cdot \mathbf{curl} \overline{\mathbf{v}_h} + \int_{\Omega} \mathbf{q}_h \cdot \overline{\mathbf{v}_h} &= \lambda_h \int_{\Omega} \mathbf{u}_h \cdot \mathbf{curl} \overline{\mathbf{v}_h}, \\ \int_{\Omega} \mathbf{u}_h \cdot \overline{\mathbf{p}_h} &= 0 \end{aligned}$$

for all  $(\mathbf{v}_h, \mathbf{p}_h) \in \mathcal{Z}_{\mathcal{I},h} \times \mathcal{H}_{\mathcal{I},h}$ .

Let  $\lambda$  be an eigenvalue of Problem 2 with multiplicity  $m$  and  $\mathcal{E} \subset \mathcal{Z}_{\mathcal{I}}$  the corresponding eigenspace. Then, there exist exactly  $m$  eigenvalues  $\lambda_h^{(1)}, \dots, \lambda_h^{(m)}$  of Problem 3 (repeated according to their respective multiplicities) which converge to  $\lambda$  as  $h \rightarrow 0$ .

Let  $\mathcal{E}_h$  be the direct sum of the eigenspaces corresponding to  $\lambda_h^{(1)}, \dots, \lambda_h^{(m)}$  and let us introduce the so-called gap between the continuous and discrete eigenspaces, given by

$$\widehat{\delta}(\mathcal{E}, \mathcal{E}_h) := \max\{\delta(\mathcal{E}, \mathcal{E}_h), \delta(\mathcal{E}_h, \mathcal{E})\},$$

with  $\delta(M, N) := \sup_{\substack{x \in M \\ \|x\|=1}} \text{dist}(x, N)$ . Then, it follows that  $\widehat{\delta}(\mathcal{E}, \mathcal{E}_h) \rightarrow 0$  as  $h$  goes to zero. Finally, the following estimates hold true (it is Theorem 2 in [2].)

**THEOREM 3.2.** *Let  $s > 0$  be such that  $\mathcal{E} \subset H^s(\mathbf{curl}; \Omega)$ . There exist constants  $C_1, C_2 > 0$ , independent of  $h$ , such that, for small  $h$ ,*

$$(3.6) \quad \widehat{\delta}(\mathcal{E}, \mathcal{E}_h) \leq C_1 h^{\min\{s,r\}},$$

and

$$(3.7) \quad |\lambda - \lambda_h^{(i)}| \leq C_2 h^{2 \min\{s,r\}}, \quad i = 1, \dots, m.$$

Once we know basis for  $\mathcal{Z}_{\mathcal{I},h}$  and  $\mathcal{H}_{\mathcal{I},h}$ , after assembling the matrices corresponding to Problem 3, we obtain an algebraic generalized eigenvalue problem of the form:

$$(3.8) \quad \begin{pmatrix} \mathbf{A} & \mathbf{B}^T \\ \mathbf{B} & \mathbf{0} \end{pmatrix} \begin{pmatrix} \vec{\mathbf{u}} \\ \vec{\mathbf{q}} \end{pmatrix} = \lambda_h \begin{pmatrix} \mathbf{C} & \mathbf{0} \\ \mathbf{0} & \mathbf{0} \end{pmatrix} \begin{pmatrix} \vec{\mathbf{u}} \\ \vec{\mathbf{q}} \end{pmatrix},$$

where  $\vec{\mathbf{u}}$  and  $\vec{\mathbf{q}}$  are the coefficients in the above given basis of  $\mathbf{u}_h$  and  $\mathbf{q}_h$ , respectively. We observe that both matrices are symmetric, but none is positive definite. However, in [10, Proposition 2] it was proved that  $(\lambda_h, \vec{\mathbf{u}}, \vec{\mathbf{q}})$  is a solution of (3.8) if and only if  $\vec{\mathbf{q}} = \mathbf{0}$  and  $(\lambda_h, \vec{\mathbf{u}})$  is a solution of the following problem:

$$(3.9) \quad (\mathbf{A} + \mathbf{B}^T \mathbf{B}) \vec{\mathbf{u}} = \lambda_h \mathbf{C} \vec{\mathbf{u}}.$$

The above is a well-posed generalized matrix eigenvalue problem with a real symmetric and positive definite left-hand side matrix and a real symmetric right-hand side matrix. According to this fact, in [10] was implemented (3.9) instead of (3.8).

**4. An equivalent reduced algebraic eigenvalue problem.** Let us assume that we know  $\{\mathbf{w}_{h,l}\}_{l=1}^{d_{\mathcal{H}_{\mathcal{I}}}}$  a basis of  $\mathcal{H}_{\mathcal{I},h}$ , and  $\{\mathbf{z}_{h,l}\}_{l=1}^{d_{\mathcal{Z}_{\mathcal{I}}}}$  a basis of  $\mathcal{Z}_{\mathcal{I},h}$  that contains it. Without loss of generality we can assume that  $\mathbf{z}_{h,l} = \mathbf{w}_{h,l}$  for  $l = 1, \dots, d_{\mathcal{H}_{\mathcal{I}}}$ .

In this way any function of  $\mathbf{v}_h \in \mathcal{Z}_{\mathcal{I},h}$  can be decomposed uniquely as the sum of  $\mathbf{v}_{h,a} \in \mathcal{H}_{\mathcal{I},h}$  plus  $\mathbf{v}_{h,b} \in \text{Span}\{\mathbf{z}_{h,l}\}_{l=d_{\mathcal{H}_{\mathcal{I}}+1}}^{d_{\mathcal{Z}_{\mathcal{I}}}} =: \mathcal{H}_{\mathcal{I},h}^c$ .

Recalling that the entries of  $\mathbf{A} \in \mathbb{R}^{d_{\mathcal{Z}_{\mathcal{I}}} \times d_{\mathcal{Z}_{\mathcal{I}}}}$  are  $a_{l,k} = \int_{\Omega} \mathbf{curl} \mathbf{z}_{h,k} \cdot \mathbf{curl} \mathbf{z}_{h,l}$ , the entries of  $\mathbf{C} \in \mathbb{R}^{d_{\mathcal{Z}_{\mathcal{I}}} \times d_{\mathcal{Z}_{\mathcal{I}}}}$  are  $c_{l,k} = \int_{\Omega} \mathbf{z}_{h,k} \cdot \mathbf{curl} \mathbf{z}_{h,l}$ , and the entries of  $\mathbf{B} \in \mathbb{R}^{d_{\mathcal{H}_{\mathcal{I}}} \times d_{\mathcal{Z}_{\mathcal{I}}}}$  are  $b_{k,l} = \int_{\Omega} \mathbf{z}_{h,k} \cdot \mathbf{z}_{h,l}$ , for a basis of  $\mathcal{Z}_{\mathcal{I},h}$  that extends a basis of  $\mathcal{H}_{\mathcal{I},h}$  we obtain

$$\mathbf{A} = \begin{pmatrix} 0 & 0 \\ 0 & \mathbf{A}_{b,b} \end{pmatrix} \quad \mathbf{C} = \begin{pmatrix} 0 & 0 \\ 0 & \mathbf{C}_{b,b} \end{pmatrix} \quad \mathbf{B} = \begin{pmatrix} \mathbf{B}_{a,a} & \mathbf{B}_{a,b} \end{pmatrix}.$$

The symmetric square matrices  $\mathbf{A}_{b,b}$  and  $\mathbf{C}_{b,b}$  have dimension  $d_{\mathcal{Z}_{\mathcal{I}}} - d_{\mathcal{H}_{\mathcal{I}}}$ . In particular  $\mathbf{A}_{b,b}$  is symmetric positive definite. In fact, if  $\vec{\mathbf{v}} \in \mathbb{R}^{d_{\mathcal{Z}_{\mathcal{I}}} - d_{\mathcal{H}_{\mathcal{I}}}}$  then  $\mathbf{v}_h = \sum_{i=1}^{d_{\mathcal{Z}_{\mathcal{I}}} - d_{\mathcal{H}_{\mathcal{I}}}} v_i \mathbf{z}_{h,d_{\mathcal{H}_{\mathcal{I}}}+i} \in \mathcal{Z}_{\mathcal{I},h}$  and  $\vec{\mathbf{v}}^T \mathbf{A}_{b,b} \vec{\mathbf{v}} = \|\mathbf{curl} \mathbf{v}_h\|_{[L^2(\Omega)]^3}^2 \geq 0$ . If  $\mathbf{A}_{b,b} \vec{\mathbf{v}} = \vec{\mathbf{0}}$  then  $\mathbf{curl} \mathbf{v}_h = \mathbf{0}$ , hence  $\mathbf{v}_h \in \mathcal{H}_{\mathcal{I},h}$  and  $\vec{\mathbf{v}} = \vec{\mathbf{0}}$ . The submatrix  $\mathbf{B}_{a,a} \in \mathbb{R}^{d_{\mathcal{H}_{\mathcal{I}}} \times d_{\mathcal{H}_{\mathcal{I}}}}$  is the mass matrix for the basis  $\{\mathbf{w}_{h,i}\}_{i=1}^{d_{\mathcal{H}_{\mathcal{I}}}}$  of  $\mathcal{H}_{\mathcal{I},h}$  hence it is symmetric positive definite.

This means that the generalised eigenvalue problem (3.8) takes the form:

$$\begin{pmatrix} 0 & 0 & \mathbf{B}_{a,a}^T \\ 0 & \mathbf{A}_{b,b} & \mathbf{B}_{a,b}^T \\ \mathbf{B}_{a,a} & \mathbf{B}_{a,b} & 0 \end{pmatrix} \begin{pmatrix} \vec{\mathbf{u}}_a \\ \vec{\mathbf{u}}_b \\ \vec{\mathbf{q}} \end{pmatrix} = \lambda_h \begin{pmatrix} 0 & 0 & 0 \\ 0 & \mathbf{C}_{b,b} & 0 \\ 0 & 0 & 0 \end{pmatrix} \begin{pmatrix} \vec{\mathbf{u}}_a \\ \vec{\mathbf{u}}_b \\ \vec{\mathbf{q}} \end{pmatrix}.$$

From the first block of equations,  $\mathbf{B}_{a,a}^T \vec{\mathbf{q}} = \vec{\mathbf{0}}$ , it follows that  $\vec{\mathbf{q}} = \vec{\mathbf{0}}$ . Then the second block reads

$$(4.1) \quad \mathbf{A}_{b,b} \vec{\mathbf{u}}_b = \lambda_h \mathbf{C}_{b,b} \vec{\mathbf{u}}_b.$$

From the third block of equations,  $\mathbf{B}_{a,a} \vec{\mathbf{u}}_a + \mathbf{B}_{a,b} \vec{\mathbf{u}}_b = \mathbf{0}$ , one has  $\vec{\mathbf{u}}_a = -\mathbf{B}_{a,a}^{-1} \mathbf{B}_{a,b} \vec{\mathbf{u}}_b$ .

We study in the sequel how to construct such a basis of  $\mathcal{Z}_{\mathcal{I},h}$  with the aid of a tree-cotree decomposition of the degrees of freedom of  $\mathcal{N}_h^r$ . We will use some elementary results of graph theory that can be found, for instance, in [17]. This kind of decomposition is well known when using finite elements of the lowest degree. In this case the degrees of freedom in  $\mathcal{N}_h^1$  are the line integrals on the edges of the mesh, and the degrees of freedom in the space of Lagrangian finite elements of degree one,  $\mathcal{L}_h^1$ , the values at the vertices of the mesh. In the following, for the sake of simplicity we consider the case  $r = 1$ . The general case  $r \geq 1$  is discussed in Appendix A.

**4.1. A basis of  $\mathcal{Z}_{\mathcal{I},h}$ .** We recall that  $\mathbf{V}_h$  is the set of vertices of  $\mathcal{T}_h$  and, with a slight abuse of notation, we denote  $\mathbf{E}_h$  the set of *oriented* edges of the mesh. We denote by  $\mathcal{T}_h^\Gamma$  the triangulation induced on  $\Gamma$  by  $\mathcal{T}_h$ . We also denote  $\mathbf{V}_h^\Gamma$ ,  $\mathbf{E}_h^\Gamma$ , and  $\mathbf{F}_h^\Gamma$  the set of vertices, oriented edges and oriented faces of  $\mathcal{T}_h^\Gamma$ , respectively.

Let  $\{\Phi_{h,i}\}_{i=1}^{d_L}$  and  $\{\omega_{h,k}\}_{k=1}^{d_N}$  be the canonical basis of  $\mathcal{L}_h^1$  and  $\mathcal{N}_h^1$  respectively. This means that  $\Phi_{h,i}(P_j) = \delta_{i,j}$  for all  $P_j \in \mathbf{V}_h$  and similarly,  $\int_{e_l} \omega_{h,k} \cdot \mathbf{t}_{e_l} = \delta_{k,l}$  for all  $e_l \in \mathbf{E}_h$ .

If  $\beta_2(\Omega) = p$ , namely,  $\Gamma = \cup_{s=0}^p \Gamma_s$  then for  $s \in \{0, \dots, p\}$  we denote

$$\mathbf{l}_{L,s} := \{j \in \{1, \dots, d_L\} : Q_j \in \Gamma_s\},$$

$$\mathbf{l}_{L,\Gamma} = \cup_{s=0}^p \mathbf{l}_{L,s},$$

$$\mathbf{l}_{L,int} := \{j \in \{1, \dots, d_L\} : Q_j \notin \Gamma\} = \{1, \dots, d_L\} \setminus \mathbf{l}_{L,\Gamma},$$

and  $d_{L,s}$ ,  $d_{L,\Gamma}$ ,  $d_{L,int}$  their respective cardinality. Similarly we denote

$$\begin{aligned} \mathsf{l}_{N,\Gamma} &:= \{l \in \{1, \dots, d_N\} : e_l \subset \Gamma\}, \\ \mathsf{l}_{N,int} &:= \{l \in \{1, \dots, d_N\} : e_l \not\subset \Gamma\} = \{1, \dots, d_N\} \setminus \mathsf{l}_{N,\Gamma}, \end{aligned}$$

and  $d_{N,\Gamma}$ ,  $d_{N,int}$  their respective cardinality.

Then  $\mathsf{V}_h^\Gamma = \{P_j\}_{j \in \mathsf{l}_{L,\Gamma}}$  and  $\mathsf{E}_h^\Gamma = \{e_l\}_{l \in \mathsf{l}_{N,\Gamma}}$ . Moreover  $\{\boldsymbol{\omega}_{h,k}\}_{k \in \mathsf{l}_{N,int}}$  is a basis of  $\mathcal{N}_h^1 \cap H_0(\mathbf{curl}; \Omega)$  being

$$H_0(\mathbf{curl}; \Omega) := \{\mathbf{v} \in H(\mathbf{curl}; \Omega) : \mathbf{v} \times \mathbf{n} = \mathbf{0} \text{ on } \Gamma\}.$$

For  $s \in \{0, \dots, p\}$  we set  $\Psi_{h,s} = \sum_{i \in \mathsf{l}_{L,s}} \Phi_{h,i}$ . Then  $\Psi_{h,s|\Gamma_s} = 1$  and  $\Psi_{h,s|\Gamma_n} = 0$  if  $n \in \{0, \dots, p\}$  and  $s \neq n$ . It is well known that  $\mathbf{grad} \Phi_{h,i} \in \mathcal{N}_h^1 \cap H_0(\mathbf{curl}; \Omega)$  for all  $i \in \mathsf{l}_{L,int}$  and also  $\mathbf{grad} \Psi_{h,s} \in \mathcal{N}_h^1 \cap H_0(\mathbf{curl}; \Omega)$  for all  $s \in \{0, \dots, p\}$ . Moreover the set

$$\{\mathbf{grad} \Phi_{h,i}\}_{i \in \mathsf{l}_{L,int}} \cup \{\mathbf{grad} \Psi_{h,s}\}_{s=1}^p$$

is linear independent. It is in fact a basis of  $\mathcal{N}_h^1 \cap H_0(\mathbf{curl}; \Omega) \cap H(\mathbf{curl}^0; \Omega)$ . In the sequel we will complete this set to obtain a basis of  $\mathcal{N}_h^1 \cap H_0(\mathbf{curl}; \Omega)$  using a tree-cotree decomposition of the oriented graph  $\mathcal{G}_{int}$  with nodes the vertices of the mesh  $\mathcal{T}_h$  contained in  $\Omega$  plus one additional node for each connected component of  $\Gamma$ , and arcs the internal oriented edges of  $\mathcal{T}_h$ ,  $\{e_l\}_{l \in \mathsf{l}_{N,int}}$ .

If  $\Theta_h = \sum_{i=1}^{d_L} \theta_i \Phi_{h,i}$  and  $\mathbf{grad} \Theta_h = \mathbf{z}_h = \sum_{k=1}^{d_N} z_k \boldsymbol{\omega}_{h,k}$  then

$$\vec{\mathbf{z}} = \mathbf{G} \vec{\boldsymbol{\theta}},$$

being  $\vec{\boldsymbol{\theta}} \in \mathbb{R}^{d_L}$  the vector with components  $\theta_i$ ,  $\vec{\mathbf{z}} \in \mathbb{R}^{d_N}$  the vector with components  $z_k$  and  $\mathbf{G} \in \mathbb{Z}^{d_N \times d_L}$  the matrix of the gradient operator that is related with the edge-vertices connectivity of the mesh. The matrix  $\mathbf{G}^T \in \mathbb{Z}^{d_L \times d_N}$  is in fact the all-nodes incidence matrix of the oriented graph  $\mathcal{G}$  with nodes the vertices and arcs the oriented edges of the mesh  $\mathcal{T}_h$  (The all-nodes incidence matrix of a graph has a row for each node and a column for each arc. See, e.g., [17]).

If  $\beta_2(\Omega) = p$ , replacing on  $\mathbf{G}^T$  the rows corresponding to vertices on each  $\Gamma_s$  by a single row equal to their sum and removing the columns corresponding to the edges on  $\Gamma$  we obtain the all-nodes incidence matrix  $\mathbf{G}_{int}^T$  of an oriented graph  $\mathcal{G}_{int}$  with nodes the vertices in the interior of  $\Omega$  plus an additional node for each connected component of  $\Gamma$ , and arcs the oriented edges of the mesh  $\mathcal{T}_h$  that are not on  $\Gamma$ . This graph  $\mathcal{G}_{int}$  is obtained by contracting for each  $s \in \{0, 1, \dots, p\}$  the arcs of  $\mathcal{G}$  corresponding to edges on  $\Gamma_s$  to a single node. The matrix  $\mathbf{G}_{int}^T$  has dimension  $(p+1+d_{L,int}) \times d_{N,int}$ . Without lost of generality we can assume that the first  $p+1$  rows are those corresponding to the nodes in the graph  $\mathcal{G}_{int}$  associated to the connected components of  $\Gamma$ . The entries of these rows are the coefficients of  $\mathbf{grad} \Psi_{h,s} = \mathbf{grad} \left( \sum_{i \in \mathsf{l}_{L,s}} \Phi_{h,i} \right)$  in the canonical basis of basis  $\mathcal{N}_h^1$  for  $s \in \{0, \dots, p\}$ .

We recall that the all-nodes incidence matrix of a connected oriented graph is not full rank since the sum of the rows is equal to zero. Each submatrix obtained eliminating a row (that corresponds to the choice of a root node in the graph) is called an incidence matrix of the graph and it is full rank. A spanning tree of a graph is a connected subgraph that contains all the nodes of the graph and that does not contain any cycle. For each connected oriented graph the columns of an incidence matrix corresponding to the arcs on a spanning tree are linear independent so the

corresponding submatrix of the incidence matrix is invertible (see, e.g., Theorem 6.9 and Theorem 6.12 in [17]).

In the graph  $\mathcal{G}_{int}$  we choose as root node the one corresponding to  $\Gamma_0$  and we denote  $\mathbf{G}_{int,*}^T$  the corresponding incidence matrix (that has dimension  $(p + d_{L,int}) \times d_{N,int}$ ; we have eliminated the first row of the all nodes incidence matrix  $\mathbf{G}_{int}^T$ ). We consider a spanning tree  $\mathcal{S}_{int}$  of the graph  $\mathcal{G}_{int}$  and decompose  $\mathbf{G}_{int,*}^T = [\mathbf{G}_{st,*}^T \ \mathbf{G}_{ct,*}^T]$ . By  $\mathbf{G}_{st,*}^T$  we indicate the columns of the incidence matrix of the graph  $\mathcal{G}_{int}$  corresponding to the arcs in the spanning tree and by  $\mathbf{G}_{ct,*}^T$  the columns corresponding to the arcs in the co-tree. So we have ordered the elements of  $\{\boldsymbol{\omega}_{h,k}\}_{k \in I_{N,int}}$  in such a way that the first  $p + d_{L,int}$  elements are those associated to edges in the spanning tree of the graph. The remaining  $d_{N,int} - (p + d_{L,int})$  are those corresponding to the cotree. We denote  $I_{N,ct} := \{k \in I_{N,int} : e_k \notin \mathcal{S}_{int}\}$

The submatrix  $\mathbf{G}_{st,*}^T \in \mathbb{R}^{(p+d_{L,int}) \times (p+d_{L,int})}$  corresponding to the arcs in the spanning tree is non singular and then also the square matrix

$$\mathbf{M} = \begin{bmatrix} \mathbf{G}_{st,*} & \mathbf{0} \\ \mathbf{G}_{ct,*} & \mathbf{I} \end{bmatrix} \in \mathbb{R}^{d_{N,int} \times d_{N,int}},$$

where  $\mathbf{I}$  indicates the identity matrix of dimension  $d_{N,int} - (p + d_{L,int})$ , is non singular. As a direct consequence, the functions  $\{\mathbf{z}_{h,j}\}_{j=1}^{d_{N,int}} \subset \mathcal{N}_h^1$  given by

$$\mathbf{z}_{h,j} = \sum_{k=1}^{d_{N,int}} m_{k,j} \boldsymbol{\omega}_{h,k},$$

where  $m_{k,j}$  denote the entries of the matrix  $\mathbf{M}$ , are a basis of  $\mathcal{N}_h^1 \cap H_0(\mathbf{curl}; \Omega)$ . In fact these functions are linear independent because  $\mathbf{M}$  is not singular and the dimension of  $\mathcal{N}_h^1 \cap H_0(\mathbf{curl}; \Omega)$  is equal to  $d_{N,int}$ . Moreover  $\mathbf{z}_{h,s} = \mathbf{grad} \Psi_{h,s}$  for  $s \in \{1, \dots, p\}$  while  $\mathbf{z}_{h,p+i} = \mathbf{grad} \Phi_{h,i}$  with  $i \in I_{L,int}$ .

We have thus proved the following result.

PROPOSITION 4.1. *The set*

$$(4.2) \quad \{\mathbf{z}_{h,j}\}_{j=1}^{d_{N,int}} := \{\mathbf{grad} \Psi_{h,s}\}_{s=1}^p \cup \{\mathbf{grad} \Phi_{h,i}\}_{i \in I_{L,int}} \cup \{\boldsymbol{\omega}_{h,k}\}_{k \in I_{N,ct}}$$

is a basis of  $\mathcal{N}_h^1 \cap H_0(\mathbf{curl}; \Omega)$ .

The next step is to extend this set to a basis of

$$\mathcal{X}_h^0 := \left\{ \mathbf{v}_h \in \mathcal{N}_h^1 : \mathbf{curl} \mathbf{v}_h \cdot \mathbf{n} = 0 \text{ on } \Gamma, \text{ and} \right. \\ \left. \oint_{\partial \Sigma_i} \mathbf{v}_h \cdot \mathbf{t}_i = \oint_{\partial \Sigma'_i} \mathbf{v}_h \cdot \mathbf{t}'_i = 0 \ \forall i \in \{1, \dots, g\} \right\}$$

by including the gradients of the elements of the canonical basis of  $\mathcal{L}_h^1$  associated to vertices of the mesh on the boundary of  $\Omega$ . We choose a vertex  $Q_{s*}$  on each connected component  $\Gamma_s$ ,  $s \in \{0, 1, \dots, p\}$ , of  $\Gamma$ . We denote  $I_{L,s}^* = \{i \in I_{L,s} : Q_i \neq Q_{s*}\}$ .

PROPOSITION 4.2. *The set*

$$\{\mathbf{grad} \Phi_{h,i}\}_{i \in I_{L,0}^*} \cup \{\mathbf{grad} \Phi_{h,i}\}_{i \in I_{L,1}^*} \cup \dots \cup \{\mathbf{grad} \Phi_{h,i}\}_{i \in I_{L,p}^*} \cup \{\mathbf{z}_{h,j}\}_{j=1}^{d_{N,int}}$$

is a basis of the space  $\mathcal{X}_h^0$ .

*Proof.* See Proposition 4.2 in [11].  $\square$

The following result follows taking (4.2) into account.

COROLLARY 4.3. *Let us denote  $\mathbf{l}_L^* = \mathbf{l}_{L,0}^* \cup (\cup_{s=1}^p \mathbf{l}_{L,s}) \cup \mathbf{l}_{L,int}$ . The set*

$$\{\mathbf{grad} \Phi_{h,i}\}_{i \in \mathbf{l}_L^*} \cup \{\boldsymbol{\omega}_{h,k}\}_{k \in \mathbf{l}_{N,ct}}$$

is a basis of  $\mathcal{X}_h^0$ .

We complete this set to a basis of the space

$$\mathcal{X}_h := \{\mathbf{v}_h \in \mathcal{N}_h^1 : \mathbf{curl} \mathbf{v}_h \cdot \mathbf{n} = 0 \text{ on } \Gamma\}.$$

For each  $i \in \{1, \dots, g\}$  let  $\phi_{h,i} \in H^1(\Omega \setminus \Sigma_i)$  be such that  $\phi_{i,h|T} \in \mathbb{P}_1(T)$  for any  $T \in \mathcal{T}_h$  and  $[[\phi_{h,i}]]_{\Sigma_i} = 1$ . We denote  $\boldsymbol{\rho}_{h,i} = \widetilde{\mathbf{grad}} \phi_{h,i}$ . Then  $\boldsymbol{\rho}_{h,i} \in \mathcal{N}_h^1$  and  $\mathbf{curl} \boldsymbol{\rho}_{h,i} = \mathbf{0}$  in  $\Omega$ . It is worth noting that  $\phi_i - \phi_{h,i} \in H^1(\Omega \setminus \Sigma_i)$  and  $[[\phi_i - \phi_{h,i}]]_{\Sigma_i} = 0$  hence  $\phi_i - \phi_{h,i}$  admits an extension to the whole  $\Omega$  that lies in the space  $H^1(\Omega)$ ,  $\boldsymbol{\rho}_i - \boldsymbol{\rho}_{h,i}$  is a gradient and

$$(4.3) \quad \oint_{\partial \Sigma_k} \boldsymbol{\rho}_{h,i} \cdot \mathbf{t}_k = \oint_{\partial \Sigma_k} \boldsymbol{\rho}_i \cdot \mathbf{t}_k = 0 \quad \text{and} \quad \oint_{\partial \Sigma'_k} \boldsymbol{\rho}_{h,i} \cdot \mathbf{t}'_k = \oint_{\partial \Sigma'_k} \boldsymbol{\rho}_i \cdot \mathbf{t}'_k = \delta_{i,k},$$

for all  $k \in \{1, \dots, g\}$ .

Finally we associate a function of  $\widehat{\mathbf{w}}'_{h,j} \in \mathcal{N}_h^1$  to each cycle  $\gamma'_j = \partial \Sigma'_j$  with  $j \in \{1, \dots, g\}$  defined as in [2].

We consider the curves  $\gamma'^+_j := \partial \Sigma'^+_j$  and  $\gamma'^-_j := \partial \Sigma'^-_j$ . Then for  $j \in \{1, \dots, g\}$  we denote  $\xi'_{h,j} \in \mathcal{C}(\Gamma \setminus \gamma'_j)$  the function such that  $\xi'_{h,j} \in \mathbb{P}_1(f)$  for all  $f \in \mathbf{F}_h^\Gamma$ ,  $\xi'_{h,j}|_{\gamma'^+_j} = 1$ ,  $\xi'_{h,j}|_{\gamma'^-_j} = 0$  and  $\xi'_{h,j}(P) = 0$  for all  $P \in \mathbf{V}_h^\Gamma \setminus \gamma'_j$ .

For each oriented edge  $e_m \in \mathbf{E}_h^\Gamma$  we denote  $P(e_m)$  and  $Q(e_m)$  the initial and final vertices of  $e_m$ , respectively and  $\mathring{e}_m := e_m \setminus \{P(e_m), Q(e_m)\}$ . Then we set

$$c'_m(\xi'_{h,j}) := \begin{cases} \lim_{\substack{s \rightarrow Q(e_m) \\ s \in \mathring{e}_m}} \xi'_{h,j}(s) - \lim_{\substack{s \rightarrow P(e_m) \\ s \in \mathring{e}_m}} \xi'_{h,j}(s), & \text{if } \mathring{e}_m \subset \Gamma \setminus \gamma'_j, \\ 0, & \text{if } e_m \subset \gamma'_j, \end{cases}$$

and define the functions

$$\widehat{\mathbf{w}}'_{h,j} := \sum_{m \in \mathbf{l}_{N,\Gamma}} c'_m(\xi'_{h,j}) \boldsymbol{\omega}_{h,m}.$$

Figure 3 shows the edges of  $\mathbf{E}_h^\Gamma$  where the associated degree of freedom of the function  $\widehat{\mathbf{w}}'_{h,j}$  is different from zero.

It has been proved in [2] that  $\widehat{\mathbf{w}}'_{h,j} \in \mathcal{X}_h$  and that

$$\oint_{\gamma'_k} \widehat{\mathbf{w}}'_{h,j} \cdot \mathbf{t}'_k = \oint_{\partial \Sigma'_k} \widehat{\mathbf{w}}'_{h,j} \cdot \mathbf{t}'_k = 0 \quad \text{and} \quad \oint_{\gamma'_k} \widehat{\mathbf{w}}'_{h,j} \cdot \mathbf{t}'_k = \delta_{k,j}$$

for  $j, k \in \{1, \dots, g\}$ . In particular this prove that the set of functions  $\{\widehat{\mathbf{w}}'_{h,j}\}_{j=1}^g$  is linear independent.

It is worth noting that the tangential trace of  $\widehat{\mathbf{w}}'_{h,j}$  is equal to zero on all but one the connected components of  $\Gamma$  and that it is different from zero only on the connected components of  $\Gamma$  contained both  $\gamma'_j$  and  $\gamma_j$ . Hence in fact one has

$$(4.4) \quad \oint_{\partial \Sigma_k} \widehat{\mathbf{w}}'_{h,j} \cdot \mathbf{t}_k = \delta_{k,j}$$

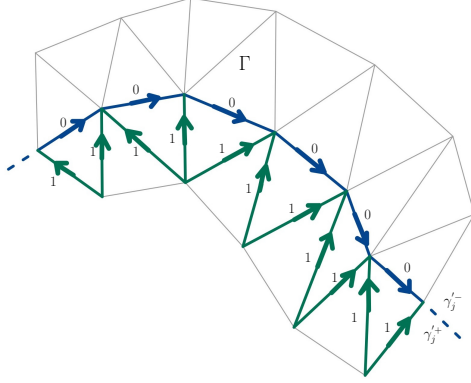


FIG. 3. In green the edges where the function  $\widehat{w}'_{h,j}$  associated to a cycle  $\gamma'_j$  has integral equal one. The integrals along all remaining edges, including those of  $\gamma'_j$  (the blue ones) are equal to zero.

for  $j, k \in \{1, \dots, g\}$ .

Now we are in position to prove the main result of this section:

PROPOSITION 4.4. *The set*

$$\{\mathbf{grad} \Phi_{h,i}\}_{i \in \mathcal{I}_L^*} \cup \{\boldsymbol{\rho}_{h,i}\}_{i \in \mathcal{I}} \cup \{\widehat{w}'_{h,j}\}_{j \in \mathcal{I}^c} \cup \{\boldsymbol{\omega}_{h,k}\}_{k \in \mathcal{I}_{N,ct}}$$

is a basis of  $\mathcal{Z}_{\mathcal{I},h}$  and the set

$$\{\mathbf{grad} \Phi_{h,i}\}_{i \in \mathcal{I}_L^*} \cup \{\boldsymbol{\rho}_{h,i}\}_{i \in \mathcal{I}}$$

is a basis of  $\mathcal{H}_{\mathcal{I},h}$ .

*Proof.* If  $\mathbf{v}_h \in \mathcal{H}_{\mathcal{I},h}$ , then from (4.3), and (4.4) one has that

$$\widehat{\mathbf{v}}_h = \mathbf{v}_h - \sum_{i \in \mathcal{I}} \left( \oint_{\partial \Sigma'_i} \mathbf{v}_h \cdot \mathbf{t}'_i \right) \boldsymbol{\rho}_{h,i} - \sum_{j \in \mathcal{I}^c} \left( \oint_{\partial \Sigma_j} \mathbf{v}_h \cdot \mathbf{t}_j \right) \widehat{w}'_{h,j}$$

belongs to  $\mathcal{X}_h^0$ . Then the first part of the result follows from Corollary 4.3. The second part follows from (4.3) and the well-known fact that  $\{\mathbf{grad} \Phi_{h,i}\}_{i \in \mathcal{I}_L^*} \cup \{\boldsymbol{\rho}_{h,i}\}_{i=1}^g$  is a basis of  $\mathcal{H}_h := \{\mathbf{v}_h \in \mathcal{N}_h^1 : \mathbf{curl} \mathbf{v}_h = \mathbf{0}\}$ .  $\square$

**5. Numerical experiments.** In this section we report some numerical tests that underline the benefits of the proposed algorithm. The algebraic generalized eigenvalue problems have been solved using the command `eigs` of MATLAB<sup>®</sup>. When computing the complete eigenfunctions the algebraic linear systems have been solved using the direct solver of MATLAB<sup>®</sup>.

**5.1. Validation of the implementation.** To validate the implementation we consider one example where the least positive eigenvalue can be computed analytically (the unit sphere). It is the smallest positive solution of the equation  $\lambda = \tan \lambda$ , namely,  $\lambda = 4.493409\dots$ , and it has multiplicity three (see [6]). Table 1 shows the three smallest positive eigenvalues of the discrete problem computed on different meshes with  $N_h$  tetrahedra, and the numerical convergence rate

$$\text{order} = -3 \frac{\log(|\lambda - \lambda_h|) / \log(|\lambda - \lambda_{h'}|)}{\log(N_h / N_{h'})}.$$

As can be seen the convergence rate is close to the theoretical one that is two.

$N_h$	$\lambda_{h,1}$	order	$\lambda_{h,2}$	order	$\lambda_{h,3}$	order
6,328	4.6529	-	4.6545	-	4.6562	-
16,539	4.5747	2.10	4.5751	2.12	4.5757	2.13
31,109	4.5450	2.15	4.5455	2.14	4.5457	2.16
65,018	4.5243	2.09	4.5243	2.13	4.5245	2.12

TABLE 1

Unit sphere. Smallest positive eigenvalues computed on different meshes and orders of convergence.

**5.2. Non-simply connected domains with connected boundary.** We consider a toroidal domain  $\Omega$  of radius  $r_1 = 1$  with circular cross section of radius  $r_2 = 0.5$  (see Figure 4 left). In this case  $\beta_1(\Omega) = 1$  and we consider  $\mathcal{I} = \emptyset$ . The exact eigenvalues are unknown so we compute corresponding extrapolated eigenvalues and an estimated convergence rate by means of a least-squares fitting of the model  $\lambda_{h,k} \approx \lambda_{\text{ex},k} + Ch^\alpha$  with  $h = N_h^{-1/3}$ .

Table 2 shows the five smallest positive eigenvalues computed on different meshes with  $N_h$  tetrahedra, the corresponding extrapolated eigenvalue  $\lambda_{\text{ex}}$  and the estimated convergence rate. It shows also the dimension of the matrix  $\mathbf{A}_{b,b}$  and the dimension of the complete matrix  $\mathbf{A}$  to quantify the reduction of the algebraic eigenvalue problem to be solved. The extrapolated eigenvalues are similar to those computed in [10] and the estimated convergence rate is again close to the theoretical one.

$N_h$	$\lambda_{h,1}$	$\lambda_{h,2}$	$\lambda_{h,3}$	$\lambda_{h,4}$	$\lambda_{h,5}$	dim $\mathbf{A}_{b,b}$	dim $\mathbf{A}$
15,554	5.0664	6.6332	6.6363	6.7097	6.7158	13,544	17,068
33,901	4.9858	6.4377	6.4405	6.5048	6.5057	30,067	37,480
65,720	4.9583	6.3720	6.3757	6.4324	6.4332	59,955	73,079
129,187	4.9314	6.3110	6.3118	6.3669	6.3676	120,272	145,056
247,239	4.9151	6.2717	6.2724	6.3256	6.3256	232,953	280,213
286,890	4.9139	6.2691	6.2696	6.3224	6.3226	269,923	323,853
$\lambda_{\text{ex}}$	4.8946	6.2283	6.2252	6.2773	6.2785	-	-
order	2.19	2.28	2.22	2.25	2.28	-	-

TABLE 2

The toroidal domain with  $\mathcal{I} = \emptyset$ . Smallest positive eigenvalues computed on different (tetrahedral) meshes.

Table 3 shows the computational time in seconds to compute five eigenvalues and corresponding eigenfunctions of the reduced generalized eigenvalue problem ( $\mathbf{A}_{b,b}$  [s. ev]), to solve the linear system to complete the eigenvalues ( $\mathbf{B}_{a,a}$  [s. ef]), and to compute five eigenvalues and eigenfunctions of the complete generalized eigenvalue problem ( $\mathbf{A}$  [s.]) (cf. (3.9)). The last column shows the ratio of the time to compute eigenvalues and eigenfunctions using the reduced system over the time using the complete system, namely  $([s. \text{ ev}] + [s. \text{ ef}]) / [s.]$ . It can be seen that the reduction of the algebraic eigenvalue problem reduce significantly the computational time even if we take into account the solution of the linear system with matrix  $\mathbf{B}_{a,a}$  necessary to compute the complete eigenfunctions. It is worth noting that this speedup increase with the dimension of the discrete problem.

In Figure 4 (right) we show the eigenfunction corresponding to the smallest positive eigenvalue that is known to be axisymmetric.

$N_h$	$\mathbf{A}_{b,b}$ [s. ev]	$\mathbf{B}_{a,a}$ [s. ef]	$\mathbf{A}$ [s.]	ratio
15,554	9.59	0.77	66.99	0.1546
33,901	24.01	2.64	261.84	0.1018
65,720	66.97	5.79	1.3189e+03	0.0552
129,187	317.09	23.75	1.4224e+04	0.0240
247,239	999.99	50.07	4.2165e+04	0.0249
286,890	1.4147e+03	76.32	9.3810e+04	0.0159

TABLE 3

The toroidal domain with  $\mathcal{I} = \emptyset$ . Computing time of eigenvalues and associated eigenfunctions by using the reduced algebraic eigenvalue problem and the complete algebraic eigenvalue problem.

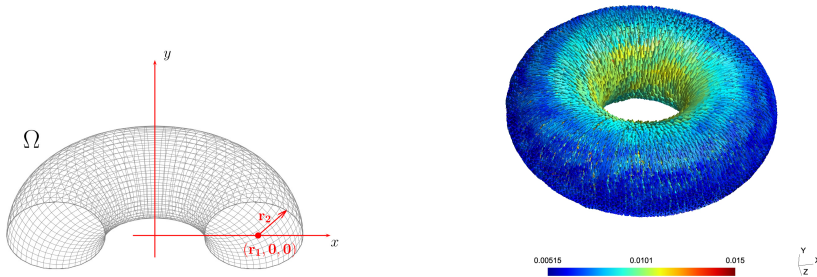


FIG. 4. The toroidal domain. On the right the eigenfunction corresponding to the smallest positive eigenvalue for  $\mathcal{I} = \emptyset$

We also consider the toroidal domain with two handles ( $\beta_1(\Omega) = 2$ ) shown in Figure 5 and already studied in [2]. In this example we choose  $\mathcal{I} = \{1\}$ . We use an hexahedral mesh as in [2]. The approximated eigenvalues computed using the proposed new basis coincide, up to the machine precision, with those computed in [2] so we show not the computed eigenvalues neither the estimate convergence rate but compare the computational cost of the two approaches.

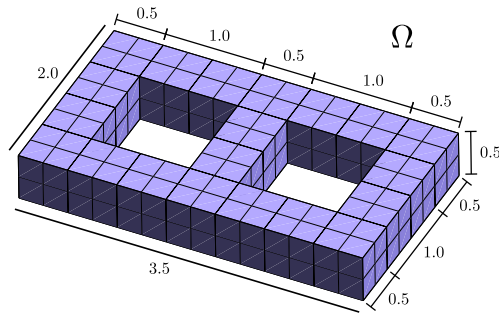


FIG. 5. The toroidal domain with two handles.

Table 4 shows the number of elements of the mesh ( $N_h$ ), the dimension of the matrix  $\mathbf{A}_{b,b}$  of the reduced algebraic eigenvalue problem ([d. ev]), and the computational time in seconds to compute six eigenpairs using the command `eigs` of MATLAB<sup>®</sup>

([s. ev]). It also shows the dimension of the matrix  $\mathbf{B}_{a,a}$  in the algebraic linear system to compute the complete eigenvectors ([d. ef]), and the computational time in seconds to solve the linear systems using the backslash command ([s. ef]). Columns [d. A] and [s. A] show the dimension of the complete eigenvalue problem, and the computational time in seconds to compute six eigenpairs of the complete eigenvalue problem. The last column shows the ratio of the time to compute eigenvalues and eigenfunctions using the reduced system over the the time using the complete system ( $([s. ev] + [s. ef]) / [s. A]$ ). It can be shown that the speedup is completely similar to the one in the case of a toroidal domain with one handle.

$N_h$	$\mathbf{A}_{b,b}$		$\mathbf{B}_{a,a}$		$\mathbf{A}$		ratio
	[d. ev]	[s. ev]	[d. ef]	[s. ef]	[d. A]	[s. A]	
1,280	1,936	2.12	1,975	0.23	3,911	17.95	0.1309
4,320	7,236	17.55	5,831	1.97	13,067	82.64	0.2362
10,240	17,984	48.8	12,879	7.6	30,863	594.97	0.0948
20,000	36,100	145.06	24,079	20.34	60,179	4.82e+03	0.0343
34,560	63,504	428.93	40,391	53.11	103,895	2.46e+04	0.0196
54,880	102,116	1.08e+03	62,775	122.88	164,891	1.05e+05	0.0144
81,920	153,856	2.06e+03	92,191	220.18	246,047	1.55e+05	0.0147

TABLE 4

A domain with two handles and  $\mathcal{I} = \{1\}$  (hexahedral mesh). Dimensions of the matrices and computing time of eigenvalues and associated eigenfunctions by using the reduced algebraic eigenvalue problem and the complete algebraic eigenvalue problem.

**5.3. The toroidal shell.** The computational domain in the last test problem is a toroidal shell, a non-simply-connected domain ( $\beta_1(\Omega) = 2$ ) with non-connected boundary ( $\beta_2(\Omega) = 1$ ). We consider two different toroidal shells. The exterior boundary is the same but the cavities are different. The cavity has square section and the length of the side of the square is  $s = 1.5$  in the first case and  $s = 0.5$  in the second one. See Figure 6.

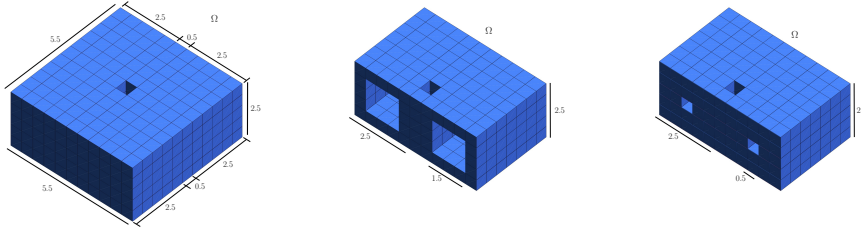


FIG. 6. The two toroidal shells: on the left the external boundary. On the center and the right a section of the domain to show the cavity in the two test cases considered.

Table 5 shows the seven smallest positive eigenvalues corresponding to  $\mathcal{I} = \{1, 2\}$ ,  $\mathcal{I} = \{1\}$ ,  $\mathcal{I} = \{2\}$ , and  $\mathcal{I} = \emptyset$  for the toroidal shell with a cavity of side  $s = 1.5$ . We indicate in boldface the eigenvalues that are not in common to all the four spectral problems. The case  $\mathcal{I} = \emptyset$  has the smallest positive eigenvalue, namely,  $\lambda_{\text{ex}} = 3.5049$ . Its inverse is the helicity of the domain.

In table 6 we show the smallest positive eigenvalue in the case  $\mathcal{I} = \emptyset$  for the two toroidal shells and the torus without cavity. The mesh is the same in the three cases and  $N_h$  is the number of elements in the mesh of the torus (without cavity). We

$\mathcal{I}$	$N_h$	$\lambda_{h,1}$	$\lambda_{h,2}$	$\lambda_{h,3}$	$\lambda_{h,4}$	$\lambda_{h,5}$	$\lambda_{h,6}$	$\lambda_{h,7}$
{1, 2}	3,072	5.6194	5.6194	6.2493	6.2493	6.5086	6.5704	6.7265
	10,368	5.1960	5.1960	5.7275	5.7275	5.9455	5.9597	6.0705
	24,576	5.0603	5.0603	5.5637	5.5637	5.7682	5.7712	5.8712
	48,000	4.9982	4.9982	5.4899	5.4899	5.6870	5.6886	5.7826
	82,944	4.9642	4.9642	5.4499	5.4499	5.6418	5.6457	5.7351
	131,712	4.9434	4.9434	5.4257	5.4257	5.6145	5.6199	5.7065
	196,608	4.9296	4.9296	5.4098	5.4098	5.5968	5.6031	5.6879
	$\lambda_{\text{ex}}$	4.8933	4.8933	5.3695	5.3695	5.5516	5.5623	<b>5.6455</b>
	rate	2.13	2.13	2.19	2.19	2.16	2.28	2.28
$\mathcal{I}$	$N_h$	$\lambda_{h,1}$	$\lambda_{h,2}$	$\lambda_{h,3}$	$\lambda_{h,4}$	$\lambda_{h,5}$	$\lambda_{h,6}$	$\lambda_{h,7}$
{1}	3,072	5.6194	5.6194	6.1080	6.2493	6.2493	6.5086	6.5704
	10,368	5.1960	5.1960	5.5793	5.7275	5.7275	5.9455	5.9597
	24,576	5.0603	5.0603	5.4152	5.5637	5.5637	5.7682	5.7712
	48,000	4.9982	4.9982	5.3416	5.4899	5.4899	5.6870	5.6886
	82,944	4.9642	4.9642	5.3019	5.4499	5.4499	5.6418	5.6457
	131,712	4.9434	4.9434	5.2778	5.4257	5.4257	5.6145	5.6199
	196,608	4.9296	4.9296	5.2621	5.4098	5.4098	5.5968	5.6031
	$\lambda_{\text{ex}}$	4.8933	4.8933	<b>5.2236</b>	5.3695	5.3695	5.5516	5.5623
	rate	2.13	2.13	2.22	2.19	2.19	2.16	2.28
$\mathcal{I}$	$N_h$	$\lambda_{h,1}$	$\lambda_{h,2}$	$\lambda_{h,3}$	$\lambda_{h,4}$	$\lambda_{h,5}$	$\lambda_{h,6}$	$\lambda_{h,7}$
{2}	3,072	5.6194	5.6194	6.2493	6.2493	6.5086	6.5704	6.7187
	10,368	5.1960	5.1960	5.7275	5.7275	5.9455	5.9597	6.0609
	24,576	5.0603	5.0603	5.5637	5.5637	5.7682	5.7712	5.8609
	48,000	4.9982	4.9982	5.4899	5.4899	5.6870	5.6886	5.7720
	82,944	4.9642	4.9642	5.4499	5.4499	5.6418	5.6457	5.7244
	131,712	4.9434	4.9434	5.4257	5.4257	5.6145	5.6199	5.6956
	196,608	4.9296	4.9296	5.4098	5.4098	5.5968	5.6031	5.6769
	$\lambda_{\text{ex}}$	4.8933	4.8933	5.3695	5.3695	5.5516	5.5623	<b>5.6345</b>
	rate	2.13	2.13	2.19	2.19	2.16	2.28	2.28
$\mathcal{I}$	$N_h$	$\lambda_{h,1}$	$\lambda_{h,2}$	$\lambda_{h,3}$	$\lambda_{h,4}$	$\lambda_{h,5}$	$\lambda_{h,6}$	$\lambda_{h,7}$
$\emptyset$	3,072	3.7098	5.6194	5.6194	6.2493	6.2493	6.5086	6.5704
	10,368	3.5931	5.1960	5.1960	5.7275	5.7275	5.9455	5.9597
	24,576	3.5538	5.0603	5.0603	5.5637	5.5637	5.7682	5.7712
	48,000	3.5358	4.9982	4.9982	5.4899	5.4899	5.6870	5.6886
	82,944	3.5261	4.9642	4.9642	5.4499	5.4499	5.6418	5.6457
	131,712	3.5202	4.9434	4.9434	5.4257	5.4257	5.6145	5.6199
	196,608	3.5164	4.9296	4.9296	5.4098	5.4098	5.5968	5.6031
	$\lambda_{\text{ex}}$	<b>3.5049</b>	4.8933	4.8933	5.3695	5.3695	5.5516	5.5623
	rate	2.07	2.13	2.13	2.19	2.19	2.16	2.28

TABLE 5

Test 3. Smallest positive eigenvalues computed on different meshes with  $\mathcal{I} = \{1, 2\}, \{1\}, \{2\}, \emptyset$ .

notice that in this case the helicity ( $H_\Omega = 1/\lambda_{\text{ex}}$ ) of the toroidal shell decrease with the dimension of the cavity and it is smaller that the helicity of the torus.

Figure 7 shows the eigenfunctions associated to the smallest eigenvalues in the two toroidal shells and the full torus with  $\mathcal{I} = \emptyset$ .

**Appendix A. High order approximation.** The extension of the construction of the basis of  $\mathcal{Z}_{\mathcal{I},h}$  to the case  $r > 1$  is straightforward using the oriented graph  $\mathcal{M}^G$  described in [1, Proposition 3.3] that has one node for each Lagrange moment and an arc for each Nédélec moment. This graph generalizes to high order approximations the graph  $\mathcal{G}$  of vertices and edges of the mesh. In fact, if  $r = 1$  the two graphs coincide. The graph  $\mathcal{M}_{int}^G$  that generalize  $\mathcal{G}_{int}$  is obtained by contracting for each  $s \in \{0, 1, \dots, p\}$  the arcs of  $\mathcal{M}^G$  corresponding to edge and face moments supported

$N_h$	$s = 1.5$	$s = 0.5$	$s = 0$
4,800	3.7098	2.0024	1.8254
16,200	3.5931	1.9843	1.8131
38,400	3.5538	1.9779	1.8088
75,000	3.5358	1.9749	1.8069
129,600	3.5261	1.9732	1.8058
205,800	3.5202	1.9722	1.8052
307,200	3.5164	1.9715	1.8048
$\lambda_{\text{ex}}$	<b>3.5049</b>	<b>1.9693</b>	<b>1.8034</b>
rate	2.07	1.95	2.01

TABLE 6

Test 3. Smallest positive eigenvalues computed on different meshes with  $\mathcal{I} = \emptyset$ .

on  $\Gamma_s$  to a single node.

Let us denote  $\{\Phi_{h,i}^r\}_{i=1}^{d_L^r}$  the canonical basis of  $\mathcal{L}_h^r$  associated to the Lagrangian moments and  $\{\omega_{h,k}^r\}_{k=1}^{d_N^r}$  the canonical basis of  $\mathcal{N}_h^r$  associated to the Nédélec moments defined as in [1, Section 3].

Corollary 4.3 holds true for  $r > 1$  replacing the set  $\{\omega_{h,k}\}_{k \in \mathcal{I}_{N,ct}}$  by the set of elements of the canonical basis of  $\mathcal{N}_h^r$ ,  $\{\omega_{h,k}^r\}_{k \in \mathcal{I}_{N,ct}}$ , corresponding to arcs in a cotree of the graph  $\mathcal{M}_{int}^G$ , and the set  $\{\mathbf{grad} \Phi_{h,i}\}_{i \in \mathcal{I}_L^*}$  by the gradients of all but one the elements of the canonical basis of  $\mathcal{L}_h^r$ ,  $\{\Phi_{h,i}^r\}_{i=1}^{d_L^r}$ . (The missing element should correspond to a moment supported on  $\Gamma$ .) A basis of  $\mathcal{X}_{\mathcal{I},h}$  is easily obtained including the functions  $\{\rho_{h,i}\}_{i \in \mathcal{I}} \cup \{\widehat{\omega}_{h,j}'\}_{j \in \mathcal{I}^c} \subset \mathcal{N}_h^1 \subset \mathcal{N}_h^r$ .

**Acknowledgements.** The research of A.A.R. is supported by the italian project PRIN201752HKH8. J.C. was partially funded by ANID-Chile projects through Fondecyt 1180859, ACE 210010 and Centro de Modelamiento Matemático (FB210005).

#### REFERENCES

- [1] A. ALONSO RODRÍGUEZ, J. CAMAÑO, E. DE LOS SANTOS, AND F. RAPETTI, *A tree-cotree splitting for the construction of divergence-free finite elements: the high-order case*. working paper or preprint, July 2019, <https://hal.archives-ouvertes.fr/hal-02429500>.
- [2] A. ALONSO RODRÍGUEZ, J. CAMAÑO, R. RODRÍGUEZ, A. VALLI, AND P. VENEGAS, *Finite element approximation of the spectrum of the curl operator in a multiply connected domain*, *Found. Comput. Math.*, 18 (2018), pp. 1493–1533, <https://doi.org/10.1007/s10208-018-9373-4>, <https://doi-org.ezp.biblio.unitn.it/10.1007/s10208-018-9373-4>.
- [3] A. BUFFA, *Hodge decompositions on the boundary of nonsmooth domains: the multi-connected case*, *Math. Models Methods Appl. Sci.*, 11 (2001), pp. 1491–1503, <https://doi.org/10.1142/S0218202501001434>, <http://dx.doi.org/10.1142/S0218202501001434>.
- [4] J. CANTARELLA, D. DETURCK, H. GLUCK, AND M. TEYTEL, *Influence of geometry and topology on helicity*, *Geophysical Monograph Series*, 111 (1999), pp. 17–24, <https://doi.org/10.1029/GM111p0017>, <https://www.scopus.com/inward/record.uri?eid=2-s2.0-40149103735&doi=10.1029%2fGM111p0017&partnerID=40&md5=bde196d0e69e1c0d426d064997819eab>. cited By 7.
- [5] J. CANTARELLA, D. DETURCK, H. GLUCK, AND M. TEYTEL, *Isoperimetric problems for the helicity of vector fields and the Biot-Savart and curl operators*, *J. Math. Phys.*, 41 (2000), pp. 5615–5641.
- [6] J. CANTARELLA, D. DETURCK, H. GLUCK, AND M. TEYTEL, *The spectrum of the curl operator on spherically symmetric domains*, *Phys. Plasmas*, 7 (2000), pp. 2766–2775, <https://doi.org/10.1063/1.874127>, <http://dx.doi.org/10.1063/1.874127>.

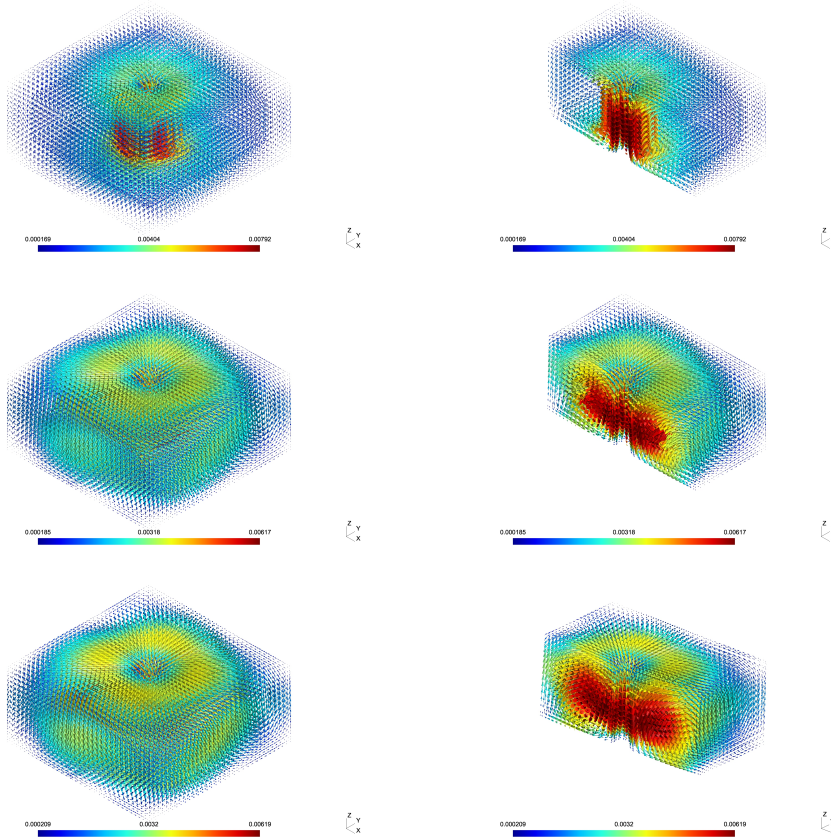


FIG. 7. The eigenfunctions associated to the smallest eigenvalues in the two toroidal shells and the full torus with  $\mathcal{I} = \emptyset$ . On the top  $s = 1.5$ , on the center  $s = 0.5$  on the bottom  $s = 0$ . On the right vertical section through the plane  $x_3 = 0$ .

- [7] C. FOIAS AND R. TEMAM, *Remarques sur les équations de Navier-Stokes stationnaires et les phénomènes successifs de bifurcation*, Ann. Scuola Norm. Sup. Pisa Cl. Sci. (4), 5 (1978), pp. 28–63.
- [8] R. HIPTMAIR, P. R. KOTIUGA, AND S. TORDEUX, *Self-adjoint curl operators*, Ann. Mat. Pura Appl. (4), 191 (2012), pp. 431–457, <https://doi.org/10.1007/s10231-011-0189-y>, <http://dx.doi.org/10.1007/s10231-011-0189-y>.
- [9] R. KRESS, *On constant-alpha force-free fields in a torus*, J. Engrg. Math., 20 (1986), pp. 323–344, <https://doi.org/10.1007/BF00044609>, <http://dx.doi.org/10.1007/BF00044609>.
- [10] E. LARA, R. RODRÍGUEZ, AND P. VENEGAS, *Spectral approximation of the curl operator in multiply connected domains*, Discrete Contin. Dyn. Syst. Ser. S, 9 (2016), pp. 235–253, <https://doi.org/10.3934/dcdss.2016.9.235>, <http://dx.doi.org/10.3934/dcdss.2016.9.235>.
- [11] S. MEDDAHI AND V. SELGAS, *A mixed-FEM and BEM coupling for a three-dimensional eddy current problem*, M2AN Math. Model. Numer. Anal., 37 (2003), pp. 291–318, <https://doi.org/10.1051/m2an:2003027>, <http://dx.doi.org/10.1051/m2an:2003027>.
- [12] H. MOFFATT, *The degree of knottedness of tangled vortex lines*, Journal of Fluid Mechanics, 35 (1969), pp. 117–129, <https://doi.org/10.1017/S0022112069000991>, <https://www.scopus.com/inward/record.uri?eid=2-s2.0-0014441553&doi=10.1017%2FS0022112069000991&partnerID=40&md5=4260285c6cbc80199c0c482bb8023867>. cited By 914.
- [13] H. K. MOFFATT, *Helicity and celestial magnetism*, Proc. A., 472 (2016), pp. 20160183, 17, <https://doi.org/10.1098/rspa.2016.0183>, <https://doi-org.ezp.biblio.unitn.it/10.1098/rspa.2016.0183>.

- [14] J.-C. NÉDÉLEC, *Mixed finite elements in  $\mathbb{R}^3$* , Numer. Math., 35 (1980), pp. 315–341.
- [15] R. PICARD, *Ein Randwertproblem in der Theorie kraftfreier Magnetfelder*, Z. Angew. Math. Phys., 27 (1976), pp. 169–180.
- [16] R. PICARD, *On a selfadjoint realization of curl and some of its applications*, Ricerche Mat., 47 (1998), pp. 153–180.
- [17] K. THULASIRAMAN AND M. SWAMY, *Graphs: theory and algorithms*, A Wiley-Interscience Publication, John Wiley & Sons, Inc., New York, 1992, <https://doi.org/10.1002/9781118033104>, <http://dx.doi.org/10.1002/9781118033104>.
- [18] A. VALLI, *A variational interpretation of the Biot-Savart operator and the helicity of a bounded domain*, J. Math. Phys., 60 (2019), pp. 021503, 7, <https://doi.org/10.1063/1.5024197>, <https://doi-org.ezp.biblio.unitn.it/10.1063/1.5024197>.
- [19] J. XIAO AND Q. HU, *An iterative method for computing Beltrami fields on bounded domains*, Tech. Report No. ICMSEC-12-15, Institute of Computational Mathematics and Scientific/Engineering Computing, Chinese Academy of Sciences, 2012. Available from: <http://www.cc.ac.cn/2012reserchreport/201215.pdf>.
- [20] Z. YOSHIDA AND Y. GIGA, *Remarks on spectra of operator rot*, Math. Z., 204 (1990), pp. 235–245, <https://doi.org/10.1007/BF02570870>, <http://dx.doi.org/10.1007/BF02570870>.

# Centro de Investigación en Ingeniería Matemática (CI<sup>2</sup>MA)

## PRE-PUBLICACIONES 2021

- 2021-17 DAVID MORA, ALBERTH SILGADO: *A  $C^1$  virtual element method for the stationary quasi-geostrophic equations of the ocean*
- 2021-18 ALFREDO BERMÚDEZ, BIBIANA LÓPEZ-RODRÍGUEZ, FRANCISCO JOSÉ PENA, RODOLFO RODRÍGUEZ, PILAR SALGADO, PABLO VENEGAS: *Numerical solution of an axisymmetric eddy current model with current and voltage excitations*
- 2021-19 RAIMUND BÜRGER, SONIA VALBUENA, CARLOS A. VEGA: *A well-balanced and entropy stable scheme for a reduced blood flow model*
- 2021-20 GABRIEL N. GATICA, CRISTIAN INZUNZA, RICARDO RUIZ-BAIER, FELIPE SANDOVAL: *A posteriori error analysis of Banach spaces-based fully-mixed finite element methods for Boussinesq-type models*
- 2021-21 DAVID MORA, IVÁN VELÁSQUEZ: *A  $C^1-C^0$  conforming virtual element discretization for the transmission eigenvalue problem*
- 2021-22 RICARDO OYARZÚA, MANUEL SOLANO, PAULO ZUÑIGA: *Analysis of an unfitted mixed finite element method for a class of quasi-Newtonian Stokes flow*
- 2021-23 FELISIA A. CHIARELLO, HAROLD D. CONTRERAS, LUIS M. VILLADA: *Nonlocal reaction traffic flow model with on-off ramps*
- 2021-24 SERGIO CAUCAO, RICARDO OYARZÚA, SEGUNDO VILLA-FUENTES, IVAN YOTOV: *A three-field Banach spaces-based mixed formulation for the unsteady Brinkman-Forchheimer equations*
- 2021-25 REINALDO CAMPOS-VARGAS, ESTHER CARRERA, BRUNO G. DEFILIPPI, CLAUDIA FUENTEALBA, IGNACIA HERNÁNDEZ, MAARTEN HERTOOG, CLAUDIO MENESES, GERARDO NUÑEZ, DIEGO PAREDES, ROMINA PEDRESCHI, VIRGILIO UARROTA: *Transcriptome and hormone analyses reveals differences in physiological age of “Hass” avocado fruit*
- 2021-26 TOMÁS BARRIOS, EDWIN BEHRENS, ROMMEL BUSTINZA: *Numerical analysis of a stabilized mixed method applied to incompressible elasticity problems with Dirichlet and with mixed boundary conditions*
- 2021-27 LILIANA CAMARGO, MANUEL SOLANO: *A high order unfitted HDG method for the Helmholtz equation with first order absorbing boundary condition*
- 2021-28 ANA ALONSO-RODRIGUEZ, JESSIKA CAMAÑO: *A graph-based algorithm for the approximation of the spectrum of the curl operator*

Para obtener copias de las Pre-Publicaciones, escribir o llamar a: DIRECTOR, CENTRO DE INVESTIGACIÓN EN INGENIERÍA MATEMÁTICA, UNIVERSIDAD DE CONCEPCIÓN, CASILLA 160-C, CONCEPCIÓN, CHILE, TEL.: 41-2661324, o bien, visitar la página web del centro: <http://www.ci2ma.udec.cl>



**CENTRO DE INVESTIGACIÓN EN  
INGENIERÍA MATEMÁTICA (CI<sup>2</sup>MA)  
Universidad de Concepción**



Casilla 160-C, Concepción, Chile  
Tel.: 56-41-2661324/2661554/2661316  
<http://www.ci2ma.udec.cl>

